Rheological study of transient networks with junctions of limited multiplicity

Tsutomu Indei[a)]
Fukui Institute for Fundamental Chemistry, Kyoto University, Kyoto 606-8103, Japan

(Received 7 November 2006; accepted 15 May 2007; published online 9 October 2007)

We theoretically study the viscoelastic and thermodynamic properties of transient gels comprised of telechelic associating polymers. We extend classical theories of transient networks so that correlations among polymer chains through the network junctions are taken into account. This extension enables us to investigate how rheological quantities such as elastic modulus, viscosity, and relaxation time are affected by the association equilibrium, and how these quantities are related to the aggregation number (or multiplicity) of the junctions. In this paper, we assume, in the conventional manner, that chains are elastically effective if both their ends are connected with other chains. It is shown that the dynamic shear moduli are well described in terms of the Maxwell model. As a result of the correlation, the reduced moduli (moduli divided by the polymer concentration) increase with the concentration, but become independent of the concentration in the high-concentration range. The fraction of pairwise junctions is larger at lower concentrations, indicating the presence of concatenated chains in the system, which decreases as the concentration increases. This leads to a network relaxation time that increases with the concentration. © *2007 American Institute of Physics*. [DOI: 10.1063/1.2747607]

I. INTRODUCTION

In some polymer gels, junctions can break and recombine in thermal fluctuations. They are called transient gels or physical gels. Most of the transient gels exhibit thermoreversible properties, i.e., they reversibly change between the gel state and the sol state as the thermodynamic conditions vary. Typically, polymers forming such thermoreversible transient gels carry a small fraction of interacting groups capable of forming bonds due to associative forces such as hydrophobic interaction, ionic association, hydrogen bonding, cross-linking by crystalline segments, and so on. Among them, hydrophobically modified water-soluble amphiphilic polymers have attracted widespread interest in recent years.[1] Amphiphilic properties stem from the hydrophilicity of the main chain and the hydrophobicity of the associative functional groups embedded in the main chain. Attractive force among the functional groups induces the formation of a transient network in aqueous media under certain thermodynamic conditions.

One of the simplest classes of associating polymers capable of forming a network includes linear polymers that have a functional group only at each of their two ends. These are called telechelic polymers. Rheological properties of these polymers have well been studied from both experimental[2–18] and theoretical[21–28] points of view with an intention of obtaining fundamental understandings of associating polymer systems. Examples of telechelic polymers are poly(ethylene oxide) (PEO) chains end capped with short alkyl groups,[2–10,12,13,15,16,27] perfluoroalkyl end-capped PEO,[11,14] and telechelic poly(*N*-isopropylacrylamide) carrying octadecyl groups at both ends.[18–20] They exhibit characteristic rheological properties, i.e., temperature-frequency superposition onto a Maxwell fluid,[3] breakdown of the Cox-Merz rule,[3,16] strain hardening,[11,16] shear thickening at relatively low shear rate followed by shear thinning,[2,3,6,11,12] etc.[16,17]

In order to investigate molecular origin of these phenomena, Tanaka and Edwards (referred to as TE in the following) developed a theory for the transient network[22,23] by extending a kinetic theory for reacting polymers.[29] Under the Gaussian chain assumption, TE succeeded to explain, for example, the linear response to the small oscillatory shear deformation described in terms of the Maxwell model with a single relaxation time. Shear thickening can also be explained by extending the TE theory so that the tension along the middle chain contains a nonlinear term.[28] We can also treat trifunctional associating polymers carrying two different species of functional groups by a straightforward extension of the TE theory.[30,31] Heretofore, several theories have been proposed to treat the dynamic properties of transient networks. For example, Wang[24] took isolated chains into consideration, and Vaccaro and Marrucci[26] incorporated the effects of incomplete relaxation of detached chains.

In all the transient network theories proposed thus far,[22–26,28,30,31] it is implicitly assumed that a fictitious network exists *a priori* [see Fig. 1(i)]. This network matrix is not a substantial one in the sense that it itself does not contribute to the elasticity of the system but plays a role as the substrate of the chains on which the association/dissociation of the end groups occurs. Chains with both their ends connected with this matrix are considered to be elastically effective. Correlations among chains are not taken into account in this treatment because each chain interacts with this matrix

[a)]Tel: +81-75-711-7834; Fax: +81-75-711-7863. Electronic mail: indei@fukui.kyoto-u.ac.jp

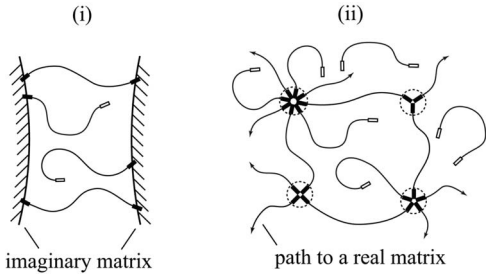

FIG. 1. (i) Drawing of the "network" postulated in the conventional transient network theories. Each chain interacts with a fictitious matrix. (ii) Schematic representation of the network considered in the present series of papers. Chains interact with each other through association/dissociation interaction among end groups. Arrows indicate paths to the (real) network matrix.

independently of the other chains, and consequently, the concentration dependence of the rheological quantities cannot be properly predicted; the elastic modulus, viscosity, etc., are simply proportional to the polymer concentration. Furthermore, it is difficult, by definition, to incorporate the information concerning the network junction, such as the aggregation number, and to study the effects of the surfactants,[32–34] single end-capped chains,[15] etc., that are added to the telechelic polymer solution.

In this series of papers, we remove this assumption and develop a theory of thermoreversible transient networks formed by multiple junctions comprising a limited number of functional groups, as depicted in Fig. 1(ii). This modification enables us to deal with the sol/gel-transition phenomenon and to predict the proper concentration dependence of rheological quantities such as the shear storage modulus G' and the loss modulus G'' in the postgel regime of the solution. In the following, we refer to the number of functional groups per junction (so-called aggregation number) as the junction multiplicity as in Ref. 35.

In the first paper of this series (this paper), we present a theoretical framework for treating such transient networks formed by multiple junctions with limited multiplicity under the assumption that chains with both their ends associated with other chains are elastically effective. That is, elastically effective chains, or active chains, are defined only locally, as in the conventional transient network theories. We derive a formula to calculate G' and G'' as a function of the frequency ω of a small applied oscillation and analyze how G' and G'', characterized by the high-frequency plateau modulus G_∞ and the relaxation time τ (and the zero-shear viscosity η_0), depend on the polymer concentration and the junction multiplicity. It is shown that the mass action law, $\psi_k = K_k(\psi_1)^k$, holds under the assumption that the connection rate of an unassociated functional group to a junction with multiplicity k (called k-junction) is proportional to the volume fraction ψ_k of the k-junctions (K_k is the reaction constant for the formation of a k-junction from k isolated functional groups). This relation is equivalent to the multiple-equilibrium condition that Tanaka and Stockmayer derived in their theory of associating polymer solutions.[35] In the second paper of this series,[36] we will incorporate the global information of the network into the definition of the active chains in order to treat the sol/gel transition and to investigate the critical behaviors of the rheological quantities near the gelation point. Looped chains, and consequently, flower micelles comprised of these loops, are assumed to be absent, for simplicity, throughout this series.

This paper is organized as follows. In Sec. II (and Appendix A), we will derive the time-evolution equation for the distribution function of chains whose one end is incorporated into a k-junction while the other end is belonging to a k'-junction. A kinetic equation for these chains will also be derived in this section (and Appendix B). Association/dissociation rates of functional groups will be introduced in Sec. III, and equilibrium properties of the system will be discussed in Sec. IV. Section V will be devoted to the study of linear rheology of the present system. Summary and discussions will be given in Sec. VI. A relation between the present theory and the TE theory will be discussed in Appendix C.

II. TIME DEVELOPMENT OF TRANSIENT NETWORKS FORMED BY JUNCTIONS WITH VARIABLE MULTIPLICITY

A. Assumptions

We consider a solution of linear polymers (or primary chains) carrying two functional groups at both their ends. Here, the functional group is a group or a short segment of the primary chain that can form aggregates (or junctions) in the solution through the noncovalent bonding. Primary chains can associate with each other through the aggregation of functional groups, while they can be detached from others due to thermal agitation or macroscopic deformations applied to the system. We assume that the association/dissociation reactions of the functional groups occur in a stepwise fashion. At equilibrium, thermodynamic conditions such as the temperature and the polymer concentration determine the association/dissociation rates of the functional groups and, hence, the number of junctions. Under certain thermodynamic conditions, primary chains construct a macroscopic network physically cross-linked by these junctions.

We allow junctions to be formed by any number of functional groups. The number of functional groups forming a junction is referred to as the junction multiplicity as in Ref. 35. We also call the junction of the multiplicity k($=1,2,3,\ldots$) the k-junction, i.e., 1-junction is an unassociated group, 2-junction is a pairwise junction, etc. For the meantime, let us identify, hypothetically, the head and tail of each chain, for convenience, by marking one of the two ends of each chain. Of course, this does not affect physical properties of the present system. Then, we term a primary chain whose head is incorporated into a k-junction and whose tail is a member of a distinct k'-junction as the (k,k')-chain. For instance, a $(k,1)$-chain ($k \geqslant 2$) is a (primary) dangling chain whose tail is not connected with other chains, and a (1,1)-chain is an isolated chain. Looped chains are assumed to be absent.

We assume that chains are elastically effective when both their ends are bound to other polymers. These chains are called active chains. Active chains are assumed to deform

affinely to the macroscopic deformation applied to the system.[40] Note that active chains are defined only locally, in the sense that they are elastically effective irrespective of whether or not the polymers they are connected with belong to the infinite network. The Rouse relaxation time τ_R of the primary chain is assumed to be much smaller than the characteristic time of a macroscopic deformation applied to the system and the lifetime of active chains, so that chains in elastically ineffective states (i.e., dangling and isolated chains) are virtually in an equilibrium state, even under flow caused by macroscopic deformation. Primary chains are assumed to be Gaussian with uniform molecular weight M (number of repeat units is N) that is smaller than the entanglement molecular weight.

B. Time-development equation for active chains

Let $F_{k,k'}(\mathbf{r},t)d\mathbf{r}$ be the number of (k,k')-chains at time t per unit volume having the head-to-tail vector $\mathbf{r}\sim\mathbf{r}+d\mathbf{r}$. Then, the total number $\nu_{k,k'}(t)$ of (k,k')-chains (per unit volume) is given by $\nu_{k,k'}(t)=\int d\mathbf{r}F_{k,k'}(\mathbf{r},t)$. Dangling and isolated chains are substantially in an equilibrium state, that is, $F_{1,k'}(\mathbf{r},t)=\nu_{1,k'}(t)f_0(\mathbf{r})$ (for $k'\geqslant 1$) and $F_{k,1}(\mathbf{r},t)=\nu_{k,1}(t)f_0(\mathbf{r})$ (for $k\geqslant 1$), where

$$f_0(\mathbf{r})\equiv\left(\frac{3}{2\pi Na^2}\right)^{3/2}\exp\left(-\frac{3|\mathbf{r}|^2}{2Na^2}\right) \tag{1}$$

is the probability distribution function (PDF) that these chains take the end-to-end vector $\mathbf{r}$ (a is the length of a repeat unit of the primary chain). The number of chains whose head (or tail) is incorporated into a k-junction is given by $\chi_k^{(h)}(t)=\Sigma_{l\geqslant 1}\nu_{k,l}(t)$ [or $\chi_k^{(t)}(t)=\Sigma_{l\geqslant 1}\nu_{l,k}(t)$]. Then, the number of chains whose one end, irrespective of whether it is the head or tail, is incorporated into a k-junction (called k-chain hereafter) is expressed as $\chi_k(t)=(\chi_k^{(h)}(t)+\chi_k^{(t)}(t))/2$, where a factor of $1/2$ is necessary to avoid double counting. The number $\mu_k(t)$ of k-junctions is obtained from the relation $\mu_k(t)=2\chi_k(t)/k$.

Due to the affine deformation assumption for active chains, the time-evolution equation for active (k,k')-chains $(k,k'\geqslant 2)$ with the head-to-tail vector $\mathbf{r}$ is expressed as

$$\frac{\partial F_{k,k'}(\mathbf{r},t)}{\partial t}+\nabla\cdot(\hat{\kappa}(t)\mathbf{r}F_{k,k'}(\mathbf{r},t)) = W_{k,k'}^{(h)}(\mathbf{r},t)+W_{k,k'}^{(t)}(\mathbf{r},t)\quad(\text{for } k,k'\geqslant 2), \tag{2}$$

where $\hat{\kappa}(t)$ is the rate of deformation tensor applied to the system, and $W_{k,k'}^{(h)}(\mathbf{r},t)$ [or $W_{k,k'}^{(t)}(\mathbf{r},t)$] is the reaction term that describes the net increase in $F_{k,k'}(\mathbf{r},t)$, per unit time, caused by the association/dissociation reactions between the head (or tail) of the (k,k')-chain and the functional groups on the other chains. The reaction term is derived according to the following procedure. The number of active (k,k')-chains decreases if (i) the head of the (k,k')-chain is dissociated from a k-junction, (ii) a functional group on the other chain is dissociated from the head of the (k,k')-chain, or (iii) an unassociated functional group connects with the head of the (k,k')-chain. On the other hand, the number of active (k,k')-chains increases if (iv) the head of the $(1,k')$-chain is connected with the $(k-1)$-junction, (v) the unassociated group of the other chain is connected with the head of the $(k-1,k')$-chain, or (vi) a functional group on the other chain is disconnected from the head of the $(k+1,k')$-chain.

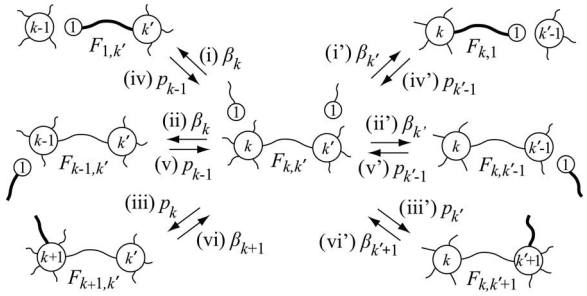

FIG. 2. Association/dissociation reactions between the functional groups on the (k,k')-chain and the functional groups on the other chains. Circles indicate junctions and lines originating from circles represent the primary chains. Character(s) inside the circle denotes the junction multiplicity. Smaller circles with 1 inside represent unassociated groups. Chains depicted by bold lines participate in the reaction. Association and dissociation rates are denoted near arrows for each reaction.

These association/dissociation reactions, (i)–(vi), are schematically depicted in Fig. 2, where the corresponding reactions regarding the tail of the (k,k')-chain, (i′)–(vi′), are also shown. Taking all these reactions into account, we obtain reaction terms as follows (see Appendix A):

$$\begin{aligned}W_{k,k'}^{(h)}(\mathbf{r},t)=&-\beta_k(r)F_{k,k'}(\mathbf{r},t)+p_{k-1}(t)F_{1,k'}(\mathbf{r},t)\\&-B_k(t)F_{k,k'}(\mathbf{r},t)+B_{k+1}(t)F_{k+1,k'}(\mathbf{r},t)\\&-P_k(t)F_{k,k'}(\mathbf{r},t)+P_{k-1}(t)F_{k-1,k'}(\mathbf{r},t),\end{aligned} \tag{3a}$$

$$\begin{aligned}W_{k,k'}^{(t)}(\mathbf{r},t)=&-\beta_{k'}(r)F_{k,k'}(\mathbf{r},t)+p_{k'-1}(t)F_{k,1}(\mathbf{r},t)\\&-B_{k'}(t)F_{k,k'}(\mathbf{r},t)+B_{k'+1}(t)F_{k,k'+1}(\mathbf{r},t)\\&-P_{k'}(t)F_{k,k'}(\mathbf{r},t)+P_{k'-1}(t)F_{k,k'-1}(\mathbf{r},t),\end{aligned} \tag{3b}$$

where we have put

$$B_k(t)\equiv(k-1)\langle\beta_k(r)\rangle(t), \tag{4a}$$

$$P_k(t)\equiv kp_k(t)\frac{\chi_1(t)}{\chi_k(t)}. \tag{4b}$$

In Eq. (4), $\beta_k(r)$ is the probability that a functional group incorporated into the k-junction $(k\geqslant 2)$ detaches itself from the junction per unit time (or dissociation rate) and $\langle\beta_k(r)\rangle$ is the expectation value of $\beta_k(r)$ averaged with respect to $\mathbf{r}$, and $p_k(t)$ is the probability that an unassociated functional group catches a k-junction per unit time (or connection rate). These rates are given in the next section.

According to the procedure described in Appendix B, the kinetic equation for the (k,k')-chains (including dangling and isolated chains) is derived as

$$\frac{d\nu_{k,k'}(t)}{dt}=w_{k,k'}(t)+w_{k',k}(t), \tag{5}$$

where, for $k'\geqslant 1$,

$$w_{k,k'}(t) = -\int d\mathbf{r}\beta_k(r)F_{k,k'}(\mathbf{r},t) + p_{k-1}(t)\nu_{1,k'}(t) - (B_k(t)+P_k(t))\nu_{k,k'}(t) + B_{k+1}(t)\nu_{k+1,k'}(t) + P_{k-1}(t)\nu_{k-1,k'}(t) \quad (\text{for } k \geqslant 2), \tag{6a}$$

$$w_{1,k'}(t) = \sum_{l\geqslant 2}\int d\mathbf{r}\beta_l(r)F_{l,k'}(\mathbf{r},t) + B_2(t)\nu_{2,k'}(t) - \left(p_1(t)+\sum_{l\geqslant 1}p_l(t)\right)\nu_{1,k'}(t). \tag{6b}$$

Summing Eq. (5) over $k' \geqslant 1$, we can obtain the kinetic equation for the k-chains as follows:

$$\frac{d\chi_k(t)}{dt} = u_k(t), \tag{7}$$

where

$$u_k(t) = -k\langle\beta_k(r)\rangle(t)\chi_k(t) + k\langle\beta_{k+1}(r)\rangle(t)\chi_{k+1}(t) + kp_{k-1}(t)\chi_1(t) - kp_k(t)\chi_1(t) \quad (\text{for } k \geqslant 2), \tag{8a}$$

$$u_1(t) = \sum_{l\geqslant 2}\langle\beta_l(r)\rangle(t)\chi_l(t) - \left(\sum_{l\geqslant 1}p_l(t)\right)\chi_1(t) + \langle\beta_2(r)\rangle(t)\chi_2(t) - p_1(t)\chi_1(t). \tag{8b}$$

One can confirm from Eq. (5) that the total number of chains is conserved, i.e., $(d/dt)\Sigma_{k\geqslant 1}\Sigma_{k'\geqslant 1}\nu_{k,k'}(t)=0$. In the following, we denote the number of total chains (per unit volume) as n, i.e., $n \equiv \Sigma_{k\geqslant 1}\Sigma_{k'\geqslant 1}\nu_{k,k'}(t)$.

III. REACTION RATES OF FUNCTIONAL GROUPS

In general, the dissociation rate of a functional group is an increasing function with respect to the chain end-to-end length r.[22,28] In the rest of this article, however, we treat the dissociation rate as a constant independent of r. This treatment is valid in the situation that the magnitude of the deformation applied to the system is so small that the change in the dissociation rate through r is also small. Then, the dissociation rate of an end group from the k-junction is supposed to take a following form: $\beta_k = \omega_0 \exp(-W_k/k_BT)$,[23] where ω_0 is a reciprocal of a microscopic time and W_k is a potential barrier for the dissociation. Here, we assume that the potential barrier does not depend on the multiplicity of the junction and set $W_k = W$ for all k. Thus, the dissociation rate also does not depend on the junction multiplicity, and is expressed as[41]

$$\beta_k = \omega_0 \exp(-W/k_BT) \equiv \beta. \tag{9}$$

The connection rate $p_k(t)$ of an unassociated group to a k-junction should increase with the number of functional groups forming k-junctions in the immediate vicinity of the unassociated group. We assume that it takes a following form:

$$p_k(t) = \omega_0 \exp(-(W-\epsilon)/k_BT)k\mu_k(t)v_0h_k, \tag{10}$$

where ϵ is a binding energy between the functional group and the junction (see Fig. 3), $k\mu_k(t)v_0$ is the number of functional groups forming k-junctions in the effective volume v_0 of the (unassociated) functional group, and h_k is a proportional factor given in the next section. It is worth noting that the connection rate depends on time through $\mu_k(t)$ in general. Equation (10) can be rewritten as

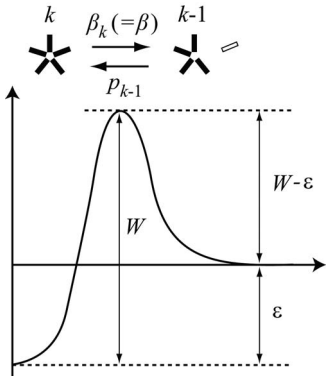

FIG. 3. The potential barrier in the vicinity of the k-junction for the association/dissociation reactions of the functional group.

$$p_k(t) = \beta\lambda(T)\psi q_k(t)h_k, \tag{11}$$

where $q_k(t) \equiv k\mu_k(t)/(2n) = \chi_k(t)/n$ is the probability that an arbitrary chosen functional group belongs to a k-junction, $\psi \equiv 2nv_0$ is the volume fraction of functional groups, and $\lambda(T) \equiv \exp(\epsilon/k_BT)$ is the association constant introduced in Ref. 35. Thus, the connection rate to the k-junction is proportional to the volume fraction $\psi q_k (\equiv \psi_k)$ of k-junctions.

IV. EQUILIBRIUM PROPERTIES

The number χ_k of k-chains, or equivalently q_k, in equilibrium can be obtained by setting Eq. (7) equal to zero. (Here and hereafter, all quantities in equilibrium are denoted without the argument t. For example, $\nu_{k,k'}$ is the number of (k,k')-chains in equilibrium.) We find that q_k is expressed as

$$q_k = \frac{p_{k-1}}{\langle\beta_k(r)\rangle}q_1 \quad (\text{for } k \geqslant 2), \tag{12}$$

where q_1 is obtained from the normalization condition, $\Sigma_{k\geqslant 1}q_k = 1$, as $q_1 = 1/(1+\Sigma_{k\geqslant 2}p_{k-1}/\langle\beta_k(r)\rangle)$. Substituting Eqs. (9) and (11) into Eq. (12), we obtain $q_k = \lambda\psi h_{k-1}q_{k-1}q_1$ for $k \geqslant 2$. By an iterating procedure, the following mass action law is derived:[42]

$$q_k = \gamma_k(\lambda\psi)^{k-1}q_1^k \quad (\text{for } k \geqslant 2), \tag{13}$$

$$q_1 = 1/\gamma(z), \tag{14}$$

where

$$\gamma_k \equiv \prod_{l=1}^{k-1} h_l \quad (\text{for } k \geqslant 2), \quad \gamma_1 \equiv 1, \tag{15}$$

$\gamma(z) \equiv \Sigma_{k\geqslant 1}\gamma_k z^{k-1}$, and $z \equiv \lambda\psi q_1$. If λ and ψ are given, then q_1 is derived by solving Eq. (14). Subsequently, we can obtain $q_k (k \geqslant 2)$ from Eq. (13). The association condition [Eq. (13)], together with Eq. (14), has been derived by Tanaka and Stockmayer (referred to as TS) from a different viewpoint in the theory of thermoreversible gelation with junctions of

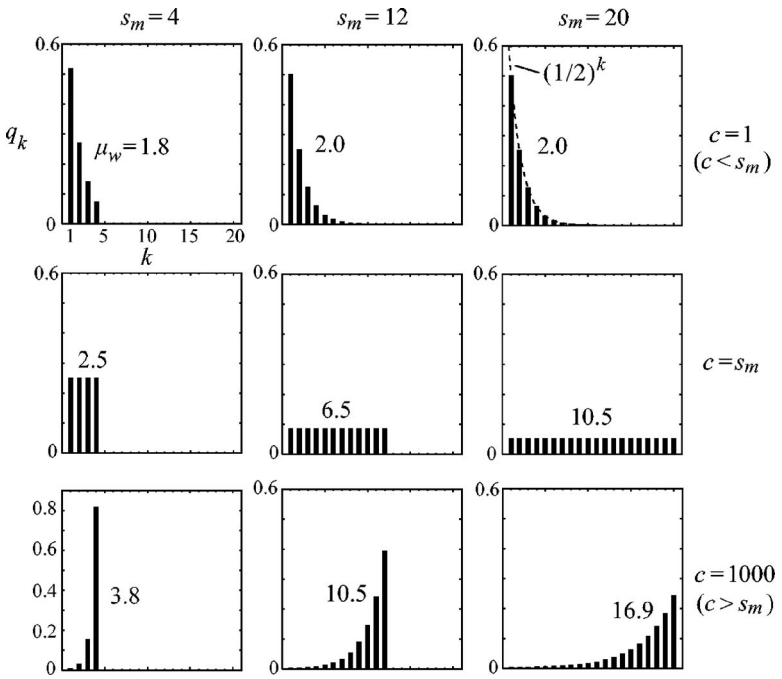

FIG. 4. The probability distribution q_k that a randomly selected functional group to be in a k-junction for the maximum multiplicity $s_m=4$ (left column), 12 (middle column), and 20 (right column), and for the reduced polymer concentration $c=1$ (top row), $c=s_m$ (middle row), $c=1000$ (bottom row). The value of the weight-average multiplicity μ_w of the junction is shown in each figure.

variable multiplicity.[35,43] In the TS theory, γ_k is interpreted as a factor giving the surface correction for the binding energy, although it is set to unity for all k for simplicity. We will adjust h_k (and hence γ_k) to derive specific models for junctions (see below). TS has shown that most quantities describing transient gels in equilibrium depend on the polymer volume fraction $\phi(=Nnv_0)$ through the combination of $\lambda(T)$ and $\psi(=2\phi/N)$. This holds not only in the equilibrium state but also under small deformations as shown in the next section. Therefore, we use $c\equiv\lambda(T)\psi$ as the reduced polymer concentration in the following. By solving an equation $d\nu_{k,k'}/dt=w_{k,k'}+w_{k',k}=0$, the number of (k,k')-chains in equilibrium is obtained as $\nu_{k,k'}=nq_kq_{k'}$.

We consider two special cases as for the multiplicity that the junction can take: (1) a saturating junction model and (2) a fixed multiplicity model. These two models have been considered by Tanaka and Stockmayer[35] in studies of the phase behavior of associating polymer solutions in equilibrium.[44] In the saturating junction model, the junction multiplicity has an upper limit s_m, that is, each junction is allowed to take a limited range $k=1,2,\ldots,s_m$ of the multiplicity. The mean multiplicity generally depends on the reduced polymer concentration in this model. On the other hand, in the fixed multiplicity model, each junction can take only one fixed multiplicity s, i.e., we have only $k=1$ (unassociated) and $k=s$ (associated) irrespective of the value of the reduced polymer concentration.

A. Saturating junction model

We can impose the upper limit on the junction multiplicity by employing h_k given by

$$h_k=\begin{cases}1 & (1\leqslant k\leqslant s_m-1)\\ 0 & (k\geqslant s_m).\end{cases} \tag{16}$$

In this case, Eq. (15) reduces to $\gamma_k=1$ (for $1\leqslant k\leqslant s_m$) and 0 $(k\geqslant s_m+1)$, and hence Eq. (13) becomes $q_k=(cq_1)^{k-1}q_1$ (for $2\leqslant k\leqslant s_m$) and 0 $(k\geqslant s_m+1)$. Thus, junctions with a multiplicity greater than s_m no longer exist. We can obtain q_1 by solving Eq. (14):

$$\frac{1}{q_1}=\frac{1-(cq_1)^{s_m}}{1-cq_1}. \tag{17}$$

The right-hand side of Eq. (17) [denoted as $g(q_1)$ for simplicity] is s_m at $q_1=1/c$. Therefore, in the case that $c=s_m$, the solution of Eq. (17) is $q_1=1/c$ $(=1/s_m)$, and hence $q_k=(cq_1)^{k-1}q_1=1/c$ for all $k(\leqslant s_m)$ (see middle row figures of Fig. 4). In the case that $s_m>c$, $g(q_1=1/c)(=s_m)$ is greater than c. This indicates that the solution of Eq. (17) satisfies a condition $q_1<1/c$, because $g(q_1)$ is an increasing function with respect to q_1. Thus, we can conclude that q_k is a decreasing function with respect to k (see top row figures of Fig. 4). In the opposite case $(s_m<c)$, the solution of Eq. (17) fulfills a condition $q_1>1/c$, and therefore q_k is an increasing function with respect to k (see bottom row figures of Fig. 4).

Figure 5(i) shows the extent of association $\alpha=1-q_1$ plotted against s_m for several values of the reduced polymer concentration c. We see that α approaches a fixed value, for each value of c, as s_m increases. This value can be estimated as follows. In an extreme case that s_m is much greater than c, the right-hand side of Eq. (17) is approximately equal to $1/(1-cq_1)$ due to the condition $cq_1<1$. It follows that $q_1\simeq 1/(1+c)$ and $\alpha\simeq c/(1+c)$. Therefore, q_k is approximately expressed as

$$q_k\simeq\frac{1}{c}\left(\frac{c}{1+c}\right)^k=\frac{1}{c}\exp[-k/\kappa]\quad(\text{for } s_m\gg c), \tag{18}$$

where $\kappa\equiv 1/\log[(1+c)/c]$ indicates the width of the distribution. As an example, Eq. (18) is plotted in Fig. 4 for the case that $c=1$ and $s_m=20$. Figure 5(ii) shows the extent of association as a function of the reduced concentration for different s_m. The extent of association behaves as $c/(1+c)$ for c much less than s_m and approaches unity as c increases.

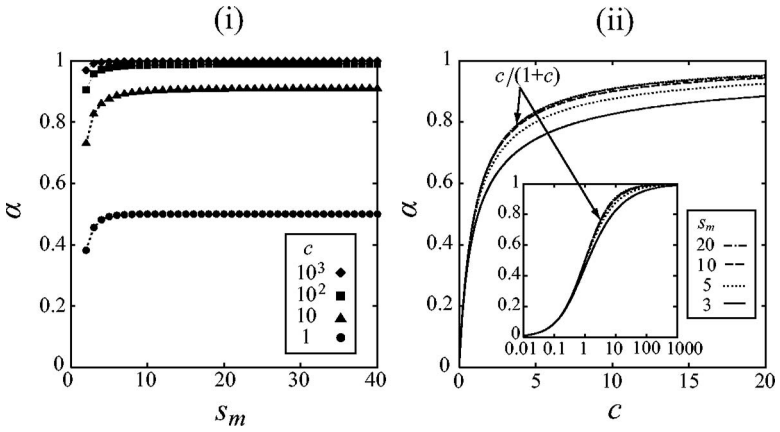

FIG. 5. The extent of association α of the saturating junction model as a function of the maximum multiplicity s_m (i) and of the reduced polymer concentration c (ii). The reduced concentration is varying from curve to curve in (i), while the maximum multiplicity is changing in (ii). The inset of (ii) shows the linear-log plot of α as a function of c. Dotted curves (behind the curves for $s_m=20$) in (ii) represent $\alpha=c/(1+c)$.

The weight-average multiplicity, defined by $\mu_w=\sum_{k=1}^{s_m}kq_k$, is shown in Fig. 4 for each set of s_m and c and plotted in Fig. 6 as a function of s_m (i) and of c (ii). It should be noted that μ_w includes unassociated groups as 1-junctions. When the reduced concentration is so small as to satisfy the condition $c \ll s_m$, then μ_w is close to $1+c$ (see also top three figures of Fig. 4). When the opposite condition ($c \gg s_m$) is fulfilled, μ_w is close to s_m (see also bottom three figures of Fig. 4) because many functional groups are incorporated into s_m-junctions.

B. Fixed multiplicity model

Let us put

$$h_k=\begin{cases}\delta & (1\leqslant k<s-1)\\ \delta^{-(s-2)} & (k=s-1)\\ 0 & (k>s-1)\end{cases} \tag{19}$$

into Eq. (13), where δ is a positive value. Then we have $q_k=(\delta c)^{k-1}q_1^k$ (for $1\leqslant k<s$), $c^{s-1}q_1^s(k=s)$, and 0 ($k>s$). In the case that δ is much less than unity, all junctions take approximately the same multiplicity s because q_k is approximately equal to zero except for the case that $k=s$ (and $k=1$), i.e., $q_k\simeq c^{s-1}q_1^s$ (for $k=s$) and 0 ($k\neq s$). It is worth noting here that it is not allowed to fix the junction multiplicity rigorously at s by setting $\delta=0$, under the assumption of stepwise reactions, because junctions with a multiplicity less than s must exist for the creation of s-junctions. In this series of papers, δ is set to 0.01. In the following, we often use the equal sign instead of the nearly equal sign ($\simeq$) for equations that approximately hold for small δ. In the fixed multiplicity model, the extent of association is given by $\alpha=q_s$ because of the normalization condition $q_1+q_s=1$.

The probability q_1 of finding an unassociated group can be obtained by solving Eq. (14):

$$\frac{1}{q_1}=1+(cq_1)^{s-1}. \tag{20}$$

The right-hand side of Eq. (20) [denoted as $g(q_1)$] is equal to 2 at $q_1=1/c$. Therefore, in the case that $c=2$, the solution of Eq. (20) is $q_1=1/2(=q_s)$. In the case that $c>2$, the solution of Eq. (20) satisfies a condition $1/c<q_1<1/2$ because $g(q_1=1/c)=2$ is less than c while $g(q_1=1/2)=1+(c/2)^{(s-1)}$ is greater than 2 [note that $g(q_1)$ is an increasing function with respect to q_1]. Thus, we can conclude that $q_s(>1/2)$ is greater than q_1, indicating that there are more associated groups in the system than unassociated ones. In the opposite case ($c<2$), the solution of Eq. (20) fulfills a condition $1/2<q_1<\min(1,1/c)$,[45] implying that $q_1>q_s$. Let us consider here an extreme case in which s is infinitely large. In the case that $c>1$, $g(q_1)$ is equal to 1 for $q_1\leqslant 1/c$ and diverges for $1/c<q_1\leqslant 1$. In the opposite case ($c\leqslant 1$), $g(q_1)$ is equal to 1 for all $q_1\leqslant 1$. Consequently, the solution of Eq. (20) is $q_1=1/c$ for $c>1$ and 1 for $c\leqslant 1$, or, equivalently, $\alpha=1-1/c$ for $c>1$ and 0 for $c\leqslant 1$. Thus, junctions suddenly appear at $c=1$ in the limit of large s. Such a sharp increase in α stems from the fact that the junctions can take (approximately) only one multiplicity; even if several functional groups spend a certain duration of time in the immediate

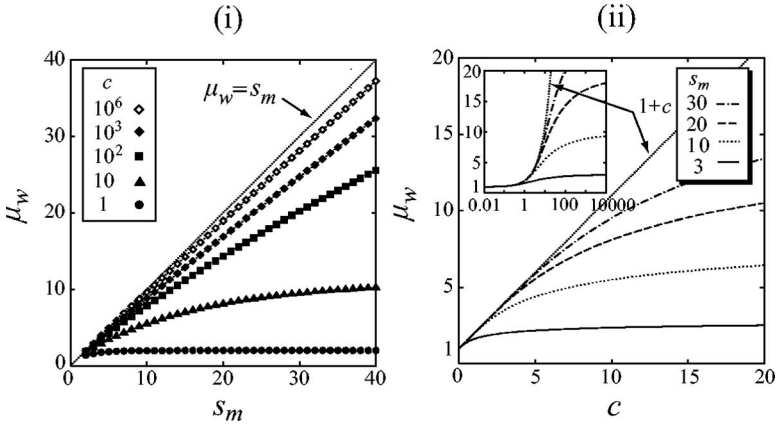

FIG. 6. The weight-average multiplicity μ_w of the junction for the saturating junction model as a function of the maximum multiplicity s_m (i) and of the reduced polymer concentration c (ii). The reduced concentration is varying from curve to curve in (i), while the maximum multiplicity is changing in (ii). The inset of (ii) shows the linear-log plot of μ_w as a function of c.

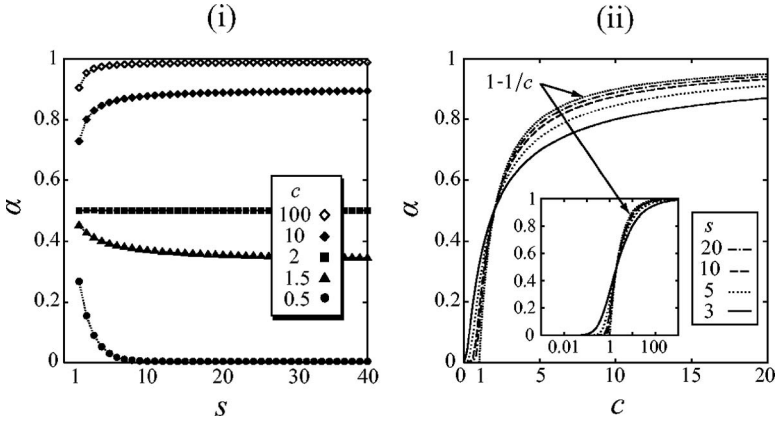

FIG. 7. The extent of association of the fixed multiplicity model as a function of the reduced polymer concentration c (i) and of the junction multiplicity s (ii). The inset of (ii) shows the linear-log plot of α as a function of c.

vicinity of each other, they cannot aggregate unless s groups participate in this event. Figure 7(i) shows the extent of association plotted against s for several c, and Fig. 7(ii) shows the extent of association as a function of c for different s. We can confirm the above-mentioned tendencies.

V. DYNAMIC-MECHANICAL AND VISCOELASTIC PROPERTIES

Now, we apply a small oscillatory shear deformation to the present system whose rate of deformation tensor is represented by

$$\hat{\kappa}(t) = \begin{pmatrix} 0 & \tilde{\epsilon}\omega\cos\omega t & 0 \\ 0 & 0 & 0 \\ 0 & 0 & 0 \end{pmatrix}, \tag{21}$$

where $\tilde{\epsilon}$ is a dimensionless infinitesimal amplitude and ω is the frequency of the oscillation. On substituting Eq. (21) into Eq. (2), the time-evolution equation becomes

$$\begin{aligned} &\frac{\partial F_{k,k'}(\mathbf{r},t)}{\partial t} + \frac{\partial F_{k,k'}(\mathbf{r},t)}{\partial x}\tilde{\epsilon}y\omega\cos\omega t \\ &= -Q_{k,k'}(t)F_{k,k'}(\mathbf{r},t) + B_{k+1}F_{k+1,k'}(\mathbf{r},t) \\ &\quad + B_{k'+1}F_{k,k'+1}(\mathbf{r},t) + P_{k-1}(t)F_{k-1,k'}(\mathbf{r},t) \\ &\quad + P_{k'-1}(t)F_{k,k'-1}(\mathbf{r},t) + \beta c(h_{k-1}q_{k-1}(t)\nu_{k',1}(t) \\ &\quad + h_{k'-1}p_{k'-1}(t)\nu_{k,1}(t))f_0(\mathbf{r}), \end{aligned} \tag{22}$$

where

$$B_k = \beta(k-1), \tag{23a}$$

$$P_k(t) = \beta z(t)kh_k \tag{23b}$$

$[z(t) \equiv \lambda\psi q_1(t)]$, and we have put

$$Q_{k,k'}(t) \equiv \beta k + P_k(t) + \beta k' + P_{k'}(t). \tag{24}$$

The number of (k,k')-chains does not depend on time for the small shear deformation,[22,23,30] and hence $\nu_{k,k'}(t)$ and $q_k(t)$ can be represented by their equilibrium values $\nu_{k,k'}$ and q_k, respectively, derived in the previous section. Here, we expand $F_{k,k'}(\mathbf{r},t)$ with respect to the powers of $\tilde{\epsilon}$ up to the first order: $F_{k,k'}(\mathbf{r},t) = F^{(0)}_{k,k'}(\mathbf{r}) + \tilde{\epsilon}F^{(1)}_{k,k'}(\mathbf{r},t)$. The zeroth-order term of $F_{k,k'}(\mathbf{r})$ represents its equilibrium value, and hence it is written as $F^{(0)}_{k,k'}(\mathbf{r}) = \nu_{k,k'}f_0(\mathbf{r})$. Comparing the order, we obtain the time-evolution equation for the first-order term $F^{(1)}_{k,k'}(\mathbf{r},t)$ as follows:

$$\begin{aligned} &\frac{\partial F^{(1)}_{k,k'}(\mathbf{r},t)}{\partial t} - \nu_{k,k'}\frac{3xy}{Na^2}f_0(\mathbf{r})\omega\cos\omega t \\ &= -Q_{k,k'}F^{(1)}_{k,k'}(\mathbf{r},t) + B_{k+1}F^{(1)}_{k+1,k'}(\mathbf{r},t) \\ &\quad + B_{k'+1}F^{(1)}_{k,k'+1}(\mathbf{r},t) + P_{k-1}F^{(1)}_{k-1,k'}(\mathbf{r},t) \\ &\quad + P_{k'-1}F^{(1)}_{k,k'-1}(\mathbf{r},t). \end{aligned} \tag{25}$$

Let us suppose that the solution of Eq. (25), in the long-time limit, takes the following form:

$$F^{(1)}_{k,k'}(\mathbf{r},t) = (g'_{k,k'}(\omega)\sin\omega t + g''_{k,k'}(\omega)\cos\omega t)\frac{3xy}{Na^2}f_0(\mathbf{r}), \tag{26}$$

where $g'_{k,k'}$ and $g''_{k,k'}$ are the in-phase and out-of-phase amplitudes of $F^{(1)}_{k,k'}(\mathbf{r},t)$, respectively, to be determined below. The subscripts of $g'^{(\prime\prime)}_{k,k'}$ are interchangeable. Substituting Eq. (26) into Eq. (25), we have the simultaneous equation for $g'^{(\prime\prime)}_{k,k'}$ $(k,k' \geqslant 2)$ as follows:

$$\begin{aligned} g'_{k,k'} = (&-Q_{k,k'}g''_{k,k'} + B_{k+1}g''_{k+1,k'} + B_{k'+1}g''_{k,k'+1} \\ &+ P_{k-1}g''_{k-1,k'} + P_{k'-1}g''_{k,k'-1})/\omega + \nu_{k,k'}, \end{aligned} \tag{27a}$$

$$\begin{aligned} g''_{k,k'} = (&Q_{k,k'}g'_{k,k'} - B_{k+1}g'_{k+1,k'} - B_{k'+1}g'_{k,k'+1} - P_{k-1}g'_{k-1,k'} \\ &- P_{k'-1}g'_{k,k'-1})/\omega. \end{aligned} \tag{27b}$$

Note that $g'^{(\prime\prime)}_{k,1} = 0$ for all $k \geqslant 1$ by definition. By solving Eq. (27), we can obtain $g'^{(\prime\prime)}_{k,k'}$ for $k,k' \geqslant 2$. In the high-frequency limit, Eq. (27) reduces to

$$g'_{k,k'}(\omega \to \infty) = \nu_{k,k'}, \tag{28a}$$

$$g''_{k,k'}(\omega \to \infty) = 0. \tag{28b}$$

The shear stress $\sigma_{k,k'}(\omega)$ originated from the (k,k')-chains is obtained from the general relation

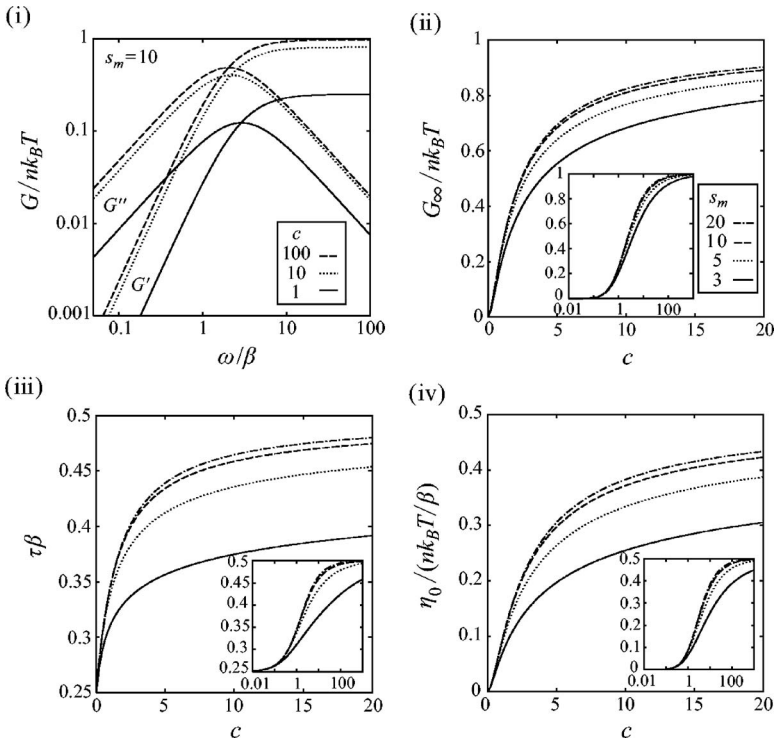

FIG. 8. (i) The reduced dynamic shear moduli for the saturating junction model as a function of the frequency. The reduced polymer concentration c is varying from curve to curve for the maximum multiplicity of the junctions fixed at $s_m=10$. (ii) The reduced plateau modulus, (iii) relaxation time, and (iv) reduced zero-shear viscosity plotted against the reduced concentration. The maximum multiplicity is varying from curve to curve. The insets of (ii)–(iv) show the linear-log plot of each quantity as a function of c.

$$\sigma_{k,k'}(\omega) = \frac{3k_BT}{Na^2}\int d\mathbf{r}xyF_{k,k'}(\mathbf{r},t)$$
$$= \bar{\epsilon}[G'_{k,k'}(\omega)\sin\omega t + G''_{k,k'}(\omega)\cos\omega t], \tag{29}$$

where the storage modulus $G'_{k,k'}(\omega)$ and the loss modulus $G''_{k,k'}(\omega)$, with regard to the (k,k')-chains, are defined by

$$G'^{(n)}_{k,k'}(\omega) \equiv k_BTg'^{(n)}_{k,k'}(\omega). \tag{30}$$

All chains whose both ends are associated with functional groups on the other chains are elastically effective, so that the total moduli $G'(\omega)$ and $G''(\omega)$ of the system can be obtained by summing Eq. (30) over $k,k'\geqslant 2$, i.e.,

$$G'^{(n)}(\omega) = k_BT\sum_{k\geqslant 2}\sum_{k'\geqslant 2} g'^{(n)}_{k,k'}(\omega). \tag{31}$$

The high-frequency plateau modulus is then found to be

$$G_\infty \equiv G'(\omega\to\infty) = \nu_0^{\mathrm{eff}}k_BT, \tag{32}$$

where

$$\nu_0^{\mathrm{eff}} = \sum_{k\geqslant 2}\sum_{k'\geqslant 2}\nu_{k,k'} = n\alpha^2 \tag{33}$$

is the total number of active chains (per unit volume).

A. Saturating junction model

We first study dynamic-mechanical and viscoelastic properties of the system in which the junctions are allowed to take a limited range $k=1,2,\ldots,s_m$ of the multiplicity. This condition can be attained by employing Eq. (16) for h_k. On substituting Eq. (16) into Eq. (23b), we obtain

$$P_k = \begin{cases} \beta zk & (1\leqslant k\leqslant s_m-1) \\ 0 & (k\geqslant s_m). \end{cases} \tag{34}$$

By substituting Eq. (34) [and Eq. (23a)] into Eq. (27) and solving a set of linear algebraic equations for $g'^{(n)}_{k,k'}$, the dynamic shear moduli can be obtained with the help of Eq. (31) in which the summation is taken over $2\leqslant k,k'\leqslant s_m$. Note that the number of unknowns in Eq. (27) is $s_m(s_m-1)$; in the case that $s_m=4$, for example, there are 12 unknowns: $g'^{(n)}_{2,2}$, $g'^{(n)}_{3,2}$, $g'^{(n)}_{3,3}$, $g'^{(n)}_{4,2}$, $g'^{(n)}_{4,3}$, and $g'^{(n)}_{4,4}$.

Figure 8(i) shows the dynamic shear moduli divided by nk_BT (reduced moduli) as a function of the frequency. The reduced polymer concentration is changed from curve to curve for the maximum multiplicity fixed at $s_m=10$. It appears that they are Maxwellian with a single relaxation time. The reduced plateau modulus (or fraction of active chains) $G_\infty/nk_BT=\nu_0^{\mathrm{eff}}/n=\alpha^2$ is plotted in Fig. 8(ii) as a function of c. When c is small, the reduced plateau modulus increases as

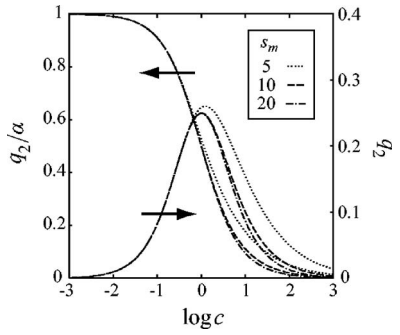

FIG. 9. The probability for a randomly selected *associated* group to be in a pairwise junction (left), and the fraction of functional groups belonging to pairwise junctions (right) plotted against the reduced polymer concentration. The maximum multiplicity of the junctions is varying from curve to curve.

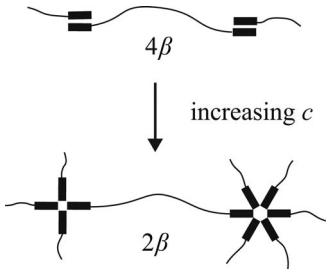

FIG. 10. The breakage rate of the active chain linking two pairwise junctions (upper figure) is 4β because the breakage rate of each pairwise junction is 2β. By contrast, the breakage rate of the active chain connecting two junctions with the multiplicity $k \geqslant 3$ (lower figure) is 2β; in other words, the chain becomes inactive if one of its two ends is dissociated from the junction.

c^2, irrespective of the value of s_m, because the extent of association is approximately equal to c [i.e., $\alpha \sim c/(1+c) \sim c$]. As c increases, G_∞/nk_BT approaches unity. Figure 8(iii) shows the relaxation time τ determined from the peak position of G''. We see that τ increases with c. This behavior can be explained as follows. As shown in Fig. 9, the probability that an associated functional group is in a pairwise junction approaches unity in the limit of a low reduced concentration. This indicates that most active chains are associated with the pairwise junctions at both their ends, thereby forming concatenated chains.[46] The breakage rate of such active chains is 4β because the annihilation rate of the pairwise junction is 2β and both ends of the chain are incorporated into the pairwise junctions. Thus, the relaxation time τ of the system approaches $1/(4\beta)$ in the limit of low c. On the other hand, τ approaches $1/(2\beta)$ with an increase in c because the fraction of the active chains connected to the junctions with a multiplicity $k \geqslant 3$ (whose breakage rate is 2β) increases, while the fraction of the active chains associated with the pairwise junctions decreases (see Fig. 10). Thus, τ increases with c. Figure 8(iv) shows the zero-shear viscosity $\eta_0 = \lim_{\omega \to 0} G''(\omega)/\omega$ divided by nk_BT/β (reduced viscosity) as a function of c. The zero-shear viscosity is roughly estimated to be $\eta_0 \sim G_\infty \tau$ [or $\eta_0/(nk_BT/\beta) \sim G_\infty/(nk_BT)\beta\tau$], and hence the reduced viscosity begins to increase at $c=0$ and approaches 0.5 as c increases.

Figure 11(i) shows the reduced shear moduli plotted against the frequency for several s_m. The reduced plateau modulus, relaxation time, and reduced zero-shear viscosity are also plotted in Fig. 11 as a function of s_m. We will now comment on the relaxation time. The relaxation time is determined from the ratio of the fraction of the active chains incorporated into the junctions with $k \geqslant 3$ to that with $k=2$ (pairwise). In the case that $s_m=2$, for example, all the active chains are associated with the pairwise junctions; consequently, the relaxation time is $\tau=1/(4\beta)$, irrespective of the value of c. With an increase in s_m, the fraction of the active chains connected to the junctions with $k=2$ decreases whereas that with $k \geqslant 3$ increases (see also Fig. 4). Thus, τ increases with s_m and approaches a fixed value for each c.

B. Fixed multiplicity model

Next, we consider the fixed multiplicity model, i.e., the multiplicity can take only $k=1$ (unassociated) and $k=s$ (associated) for all junctions. This condition can be approximately attained by employing Eq. (19) for h_k. In this case, Eq. (23b) becomes

$$P_k = \beta z k \begin{cases} \delta & (1 \leqslant k < s-1) \\ \delta^{-(s-2)} & (k = s-1) \\ 0 & (k > s-1), \end{cases} \tag{35}$$

where we are setting $\delta=0.01$. By putting Eq. (35) [and Eq. (23a)] into Eq. (27) and solving a simultaneous equation, we

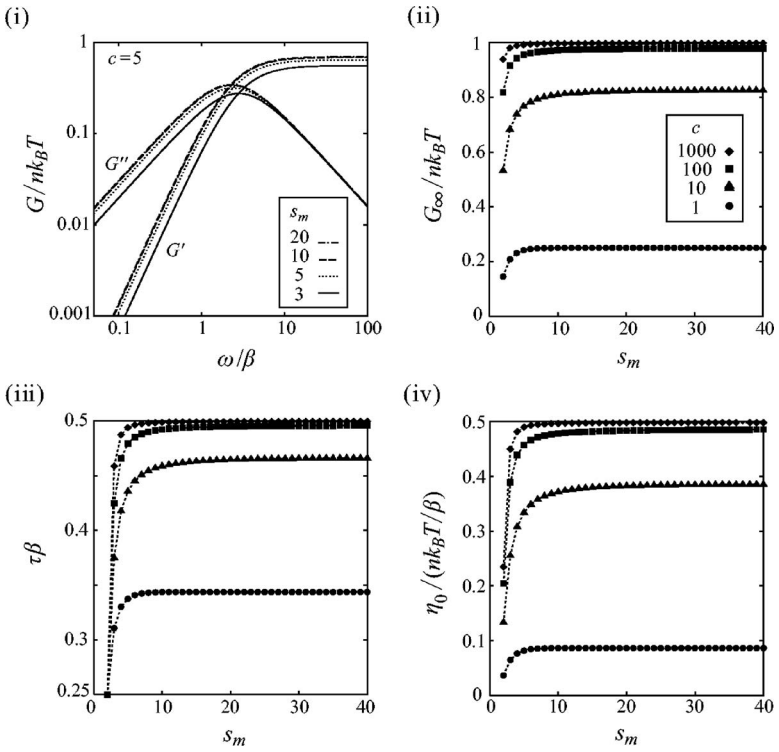

FIG. 11. (i) The reduced dynamic shear moduli for the saturating junction model as a function of the frequency. The maximum multiplicity s_m of the junctions is varying from curve to curve for the reduced polymer concentration fixed at $c=5$. (ii) The reduced plateau modulus, (iii) relaxation time, and (iv) reduced zero-shear viscosity plotted against the maximum multiplicity for several c.

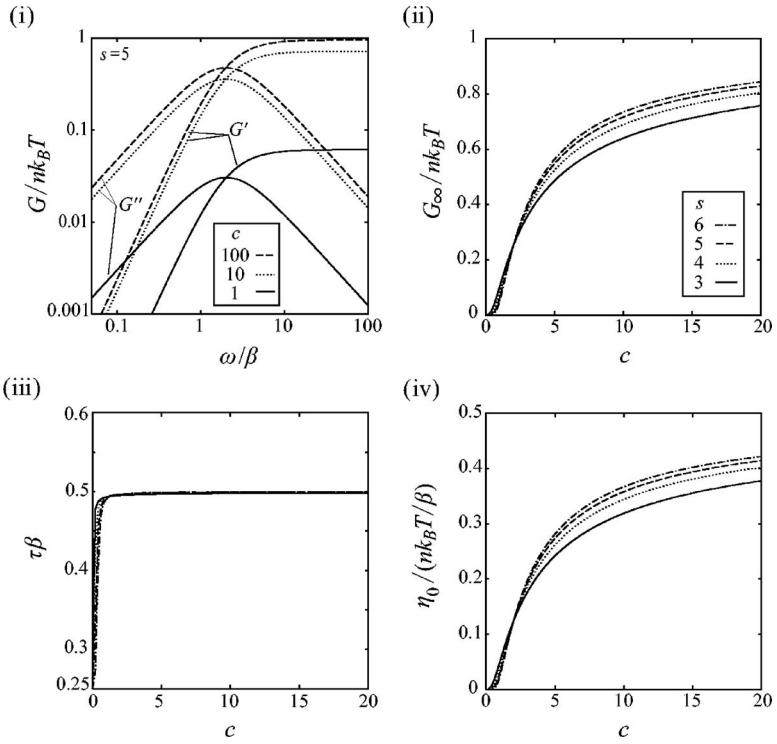

FIG. 12. (i) The reduced dynamic shear moduli for the fixed multiplicity model as a function of the frequency. The reduced polymer concentration c is varying from curve to curve for the junction multiplicity fixed at $s=5$. (ii) The reduced plateau modulus, (iii) relaxation time, and (iv) reduced zero-shear viscosity plotted against the reduced polymer concentration for different s.

can obtain the dynamic shear moduli for the fixed multiplicity model.

Figure 12 shows the dependence of the reduced shear moduli on c. The reduced plateau modulus [Fig. 12(ii)] increases with s for $c>2$ but decreases for $c<2$ according to the s dependence of α (see Fig. 7). The relaxation time [Fig. 12(iii)] is almost constant $[1/(2\beta)]$ irrespective of both the multiplicity and the reduced polymer concentration. This is because almost all junctions possess the same multiplicity which is greater than or equal to 3.[47] The reduced zero-shear viscosity [Fig. 12(iv)] is approximately half the reduced plateau modulus because $\beta\tau$ is approximately equal to 0.5.

VI. SUMMARY AND DISCUSSIONS

In this paper, we developed a theory of transient networks with multiple junctions of limited multiplicity. We assumed that the connection rate of a functional group is proportional to the volume fraction of junctions to which it is going to connect and showed that the law of mass action holds in this system, as it should be. As the first attempt, we defined active chains locally, i.e., chains whose both ends are connected with other chains are elastically effective. The dynamic shear moduli are well described in terms of the Maxwell model characterized by a single relaxation time and the high-frequency plateau modulus (and the zero-shear viscosity). They depend on thermodynamic quantities such as polymer concentration and temperature through the reduced polymer concentration c. The plateau modulus and zero-shear viscosity increase nonlinearly with c at small c and are proportional to c when c is large. In the case that the multiplicity is allowed to take any value less than a certain value (saturating junction model), the relaxation time also increases with c due to the presence of pairwise junctions at small c.

The junction multiplicity affects rheological properties of transient networks. For the saturating junction model, the dynamic shear moduli increase with the upper limit s_m of the multiplicity. The relaxation time also increases with s_m because the fraction of pairwise junctions decreases. In the case that the junction multiplicity is allowed to take only a single value s (fixed multiplicity model), the plateau modulus and zero-shear viscosity increase with s, but the relaxation time does not depend on s due to the absence of pairwise junctions.

In Fig. 13, the theoretically obtained plateau modulus, relaxation time, and zero-shear viscosity for the saturating junction model are compared with the experimental data for aqueous solutions of telechelic PEO end capped with C_{16} alkanes.[3,9] The reduced concentration c used in the theory was converted into the polymer concentration in weight percentage c_w through the relation $c=\xi c_w$, where $\xi \equiv (2000N_A/M)\lambda v_0$ (N_A is Avogadro's number). We see that, except for the relaxation time, both agree fairly well with each other for larger s_m. The deviation probably originates from the current definition of the active chains. Under this assumption, each chain linking two pairwise junctions is also elastically active. At low concentrations, there exists a large fraction of active chains of this type forming concatenated chains. In fact, however, primary chains linking two pairwise junctions should not be considered individually active; an interconnected chain comprising such primary chains should, instead, be regarded as a single active bridge (this causes overestimation of the plateau modulus at low concentrations). As indicated by Annable *et al.*,[3] such concatenated chains have shorter lifetimes than active primary chains due to the large number of possible disengagement points within the backbone. Thus, under the present assumptions, the relaxation time is overestimated at low concentrations. In order

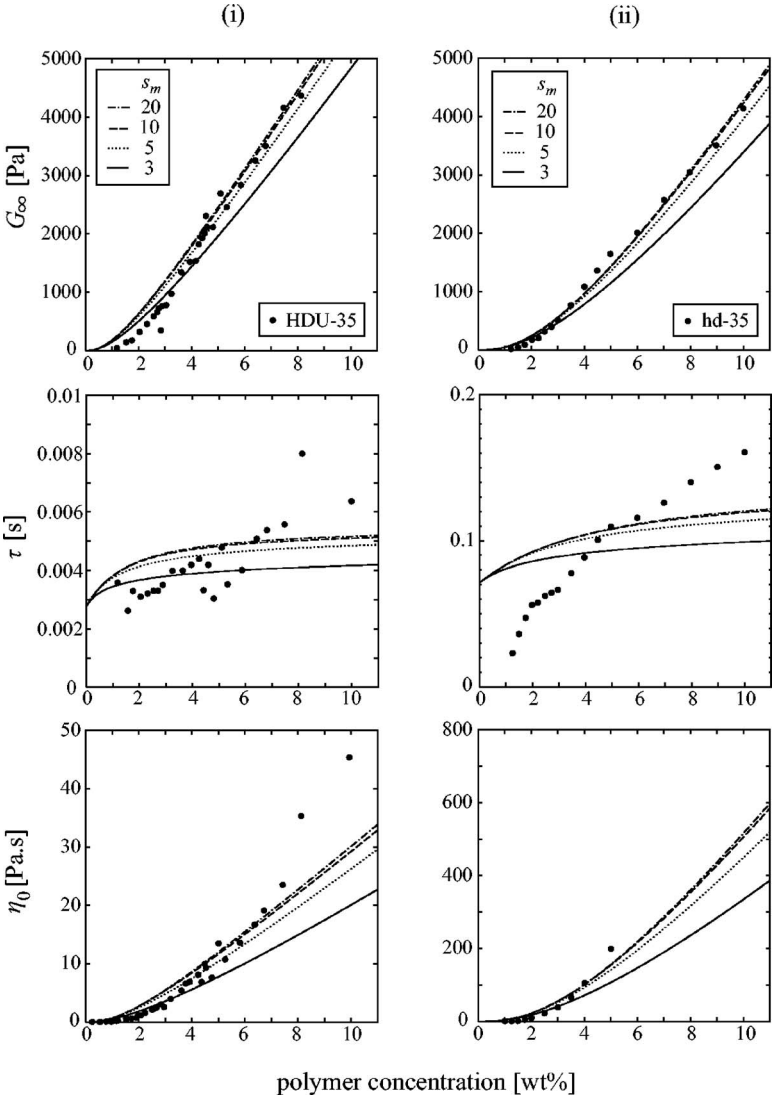

FIG. 13. Comparison between theoretical results for the saturating junction model and experimental data obtained for (i) telechelic PEO with narrow molecular weight distributions (M_w=35 kg/mol) fully end capped with C_{16} alkanes reported by Pham *et al.* (Ref. 9) (called HDU-35) and (ii) hydrophobically modified ethylene oxide-urethane copolymers (HEUR) with similar molecular weight end capped with the same hydrophobes reported by Annable *et al.* (Ref. 3) (called hd-35 after Ref. 27). Theoretical curves for the zero-shear viscosity and the relaxation time are drawn with β fixed at 90 1/s for HDU-35 and 3.5 1/s for hd-35. [A discrepancy between the values of β for the same alkanes might stem from the difference in the coupling agents between the alkanes and the PEO backbone (Refs. 9 and 27).] A factor ξ (see text) is set to 1 for HDU-35 and 0.35 for hd-35.

to treat such *superbridges* in a more appropriate manner, the global structure of the network must be taken into account with the help of a concept of the path connectivity to the network matrix.[38,39] On the other hand, in the present theory, G_∞ and η_0 (and τ) begin to increase at $c=0$, indicating that the critical concentration for the sol/gel transition is $c^*=0$. This unfavorable result is also ascribed to the lack of global information in the current theoretical treatment. The effects of superbridges on the rheological properties as well as the sol/gel transition of the transient network will be discussed in detail in the second paper of this series.[36]

APPENDIX A: DERIVATION OF REACTION TERMS

The increment in the number of (k,k')-chains with the head-to-tail vector $\mathbf{r}$ due to the dissociation reactions (i) and (ii) (see text) per unit time is written as

$$\sum_{k_h=0}^{k-1} \int \prod_{s=1}^{k_h} d\mathbf{r}_s^{(h)} \int \prod_{s'=1}^{k_t} d\mathbf{r}_s^{(t)} \left(\beta_k(r) + \sum_{s''=1}^{k_h} \beta_k(r_{s''}^{(h)}) + \sum_{s''=1}^{k_t} \beta_k(r_{s''}^{(t)}) \right) \times \mathcal{F}_{k,k'}(\mathbf{r},\{\mathbf{r}^{(h)}\},\{\mathbf{r}^{(t)}\};t), \quad \text{(A1)}$$

where the first term $\beta_k(r)$ in the parentheses stems from the dissociation reaction (i) while the second and third terms originated from reaction (ii). $\mathcal{F}_{k,k'}(\mathbf{r},\{\mathbf{r}^{(h)}\},\{\mathbf{r}^{(t)}\};t)$ is the number of (k,k')-chains with the head-to-tail vector $\mathbf{r}$ whose head is incorporated into the k-junction formed by k_h heads (and k_t tails) of the other chains each having the head-to-tail vector $\mathbf{r}_1^{(h)},\ldots,\mathbf{r}_{k_h}^{(h)}$ (and $\mathbf{r}_1^{(t)},\ldots,\mathbf{r}_{k_t}^{(t)}$) (see Fig. 14). Note that the relation $(k_h+1)+k_t=k$ holds. This quantity can be expressed as

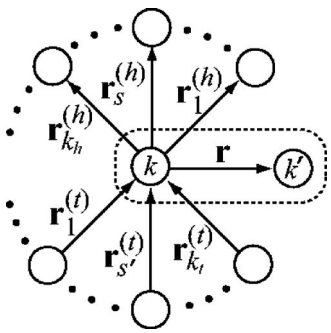

FIG. 14. The number of the states described in this figure is given by Eq. (A2). Circles stand for junctions and arrows linking two junctions represent the head-to-tail vector of the chain (chains are not shown here for simplicity).

$$\mathcal{F}_{k,k'}(\mathbf{r},\{\mathbf{r}^{(h)}\},\{\mathbf{r}^{(t)}\};t)$$
$$= C_{k_h} F_{k,k'}(\mathbf{r},t) \prod_{s=1}^{k_h} f_k^{(h)}(\mathbf{r}_s^{(h)},t) \prod_{s'=1}^{k_t} f_k^{(t)}(\mathbf{r}_{s'}^{(t)},t), \tag{A2}$$

where $f_k^{(h)}(\mathbf{r},t) \equiv \Sigma_{l\geqslant 1} F_{k,l}(\mathbf{r},t)/\Sigma_{l\geqslant 1}\nu_{k,l}(t)$ [or $f_k^{(t)}(\mathbf{r},t) \equiv \Sigma_{l\geqslant 1} F_{l,k}(\mathbf{r},t)/\Sigma_{l\geqslant 1}\nu_{l,k}(t)$] is the PDF that the chain whose head (or tail) is incorporated into a k-junction has the head-to-tail vector $\mathbf{r}$. A prefactor $C_{k_h} \equiv (1/2^{k-1})(k-1)!/(k_h!k_t!)$ is the probability that the k-junction is formed by k_h heads and k_t tails of the other chains [in addition to a head of the (k,k')-chain]. Equation (A1) reduces to

$$\beta_k(r)F_{k,k'}(\mathbf{r},t) + (k-1)\langle\beta_k(r)\rangle(t)F_{k,k'}(\mathbf{r},t), \tag{A3}$$

where $\langle\beta_k(r)\rangle(t) \equiv \int d\mathbf{r}\beta_k(r)f_k(\mathbf{r},t)$ is the expectation value of $\beta_k(r)$ averaged with respect to the PDF for the k-chains given by $f_k(\mathbf{r},t) \equiv (f_k^{(h)}(\mathbf{r},t)+f_k^{(t)}(\mathbf{r},t))/2$. The number of (k,k')-chains decreases due to the association reaction (iii) only when the k-junction, to which an unassociated group is going to connect, contains the head of the (k,k')-chain (with the head-to-tail vector $\mathbf{r}$). The decrement in $F_{k,k'}(\mathbf{r},t)$ (per unit time) as a result of reaction (iii) can be expressed as the product of the number $p_k(\chi_1^{(h)}(t)+\chi_1^{(t)}(t))$ of unassociated ends (both the head and tail) that connect to the k-junction per unit time and the number of (k,k')-chains (with the head-to-tail vector $\mathbf{r}$) per k-junction, that is,

$$p_k(t)(\chi_1^{(h)}(t)+\chi_1^{(t)}(t))\frac{F_{k,k'}(\mathbf{r},t)}{\mu_k(t)} = kp_k(t)\frac{\chi_1(t)}{\chi_k(t)}F_{k,k'}(\mathbf{r},t). \tag{A4}$$

The increment in $F_{k,k'}(\mathbf{r},t)$ caused by the association reaction (iv) is written as

$$p_{k-1}(t)F_{1,k'}(\mathbf{r},t), \tag{A5}$$

whereas the increment in $F_{k,k'}(\mathbf{r},t)$ due to the association reaction (v) is given by Eq. (A4) with k replaced by $k-1$, i.e.,

$$(k-1)p_{k-1}(t)\frac{\chi_1(t)}{\chi_{k-1}(t)}F_{k-1,k'}(\mathbf{r},t). \tag{A6}$$

The increment in $F_{k,k'}(\mathbf{r},t)$ as a result of the dissociation reaction (vi) is given by the second term of Eq. (A3) with k replaced by $k+1$, i.e.,

$$k\langle\beta_{k+1}(r)\rangle(t)F_{k+1,k'}(\mathbf{r},t). \tag{A7}$$

From Eqs. (A3)–(A7), we can obtain the reaction term [Eq. (3a)] with regard to the head of the (k,k')-chains. According to the similar procedure, the reaction term (Eq. (3b)) associated with the tail of the (k,k')-chains can be derived.

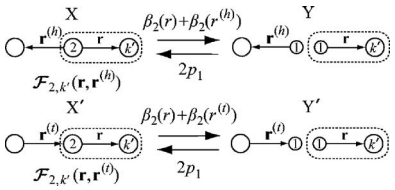

FIG. 15. Association/dissociation reactions related to the pairwise junctions.

APPENDIX B: DERIVATION OF KINETIC EQUATIONS

A kinetic equation for the (k,k')-chains is written as

$$\frac{d\nu_{k,k'}(t)}{dt} = w_{k,k'}^{(h)}(t) + w_{k,k'}^{(t)}(t), \tag{B1}$$

where $w_{k,k'}^{(h)}(t)$ and $w_{k,k'}^{(t)}(t)$ are the terms representing the net increase in the number of (k,k')-chains caused by the association/dissociation reactions which occur for the head and tail of the (k,k')-chains, respectively. With regard to active chains, these terms (for $k,k'\geqslant 2$) are obtained by simply integrating both sides of Eq. (2) with respect to $\mathbf{r}$ as follows:

$$w_{k,k'}^{(h)}(t) = -\int d\mathbf{r}\beta_k(r)F_{k,k'}(\mathbf{r},t) + p_{k-1}(t)\nu_{1,k'}(t)$$
$$- B_k(t)\nu_{k,k'}(t) + B_{k+1}(t)\nu_{k+1,k'}(t) - P_k(t)\nu_{k,k'}(t)$$
$$+ P_{k-1}(t)\nu_{k-1,k'}(t), \tag{B2a}$$

$$w_{k,k'}^{(t)}(t) = -\int d\mathbf{r}\beta_{k'}(r)F_{k,k'}(\mathbf{r},t) + p_{k'-1}(t)\nu_{k,1}(t)$$
$$- B_{k'}(t)\nu_{k,k'}(t) + B_{k'+1}(t)\nu_{k,k'+1}(t)$$
$$- P_{k'}(t)\nu_{k,k'}(t) + P_{k'-1}(t)\nu_{k,k'-1}(t). \tag{B2b}$$

The reaction terms with regard to dangling chains are $w_{1,k'}^{(h)}(t)$, $w_{1,k'}^{(t)}(t)$ (for $k'\geqslant 2$) and $w_{k,1}^{(t)}(t)$, $w_{k,1}^{(h)}(t)$ (for $k\geqslant 2$). We can derive the reaction term $w_{1,k'}^{(h)}(t)$ $(k'\geqslant 2)$ regarding the head of the $(1,k')$-chains as follows. A $(1,k')$-chain is created from a (l,k')-chain $(l\geqslant 2)$ if a head of the (l,k')-chain is detached from the l-junction. In the case that $l\geqslant 3$, the increment in the number $\nu_{1,k'}$ of $(1,k')$-chains due to this dissociation reaction (per unit time) is $\Sigma_{l\geqslant 3}\int d\mathbf{r}\beta_l(r)F_{l,k'}(\mathbf{r},t)$. In the case that $l=2$, a $(1,k')$-chain is generated if the head of the $(2,k')$-chain *or* an end group (head or tail) of another chain is detached from the $l=2$-junction (see Fig. 15). The increment in $\nu_{1,k'}$ caused by the transition from state X shown in Fig. 15 to Y is expressed as

$$\int d\mathbf{r}\int d\mathbf{r}^{(h)}(\beta_2(r)+\beta_2(r^{(h)}))\mathcal{F}_{2,k'}(\mathbf{r},\mathbf{r}^{(h)};t)$$
$$= \frac{1}{2}\int d\mathbf{r}\beta_2(r)F_{2,k'}(\mathbf{r},t)$$
$$+ \frac{1}{2}\left(\int d\mathbf{r}\beta_2(r)f_2^{(h)}(\mathbf{r},t)\right)\nu_{2,k'}(t). \tag{B3}$$

Similarly, the increment in $\nu_{1,k'}$ as a result of the transition from the state X′ (see Fig. 15) to Y′ is

$$\frac{1}{2}\int d\mathbf{r}\beta_2(r)F_{2,k'}(\mathbf{r},t)+\frac{1}{2}\left(\int d\mathbf{r}\beta_2(r)f_2^{(t)}(\mathbf{r},t)\right)\nu_{2,k'}(t). \tag{B4}$$

A $(1,k')$-chain is annihilated if its unassociated head captures a l-junction ($l\geqslant 1$). In the case that $l\geqslant 2$, the decrement in $\nu_{1,k'}$ is written as $(\Sigma_{l\geqslant 2}p_l(t))\nu_{1,k'}(t)$. In the case that $l=1$, the decrement in $\nu_{1,k'}(t)$ is expressed as $2p_1(t)\nu_{1,k'}(t)$ (see Fig. 15). Considering all these terms, we obtain

$$w_{1,k'}^{(h)}(t)=\sum_{l\geqslant 2}\int d\mathbf{r}\beta_l(r)F_{l,k'}(\mathbf{r},t)-\left(\sum_{l\geqslant 1}p_l(t)\right)\nu_{1,k'}(t)+B_2(t)\nu_{2,k'}(t)-p_1(t)\nu_{1,k'}(t). \tag{B5}$$

The reaction term $w_{1,k'}^{(t)}(t)$ ($k'\geqslant 2$) regarding the tail of the $(1,k')$-chains is given by Eq. (B2b) with k set equal to unity. According to the similar procedure, the reaction term $w_{k,1}^{(t)}(t)$ relating to the tail of the $(k,1)$-chains ($k\geqslant 2$) is obtained as

$$w_{k,1}^{(t)}(t)=\sum_{l\geqslant 2}\int d\mathbf{r}\beta_l(r)F_{k,l}(\mathbf{r},t)-\left(\sum_{l\geqslant 1}p_l(t)\right)\nu_{k,1}(t)+B_2(t)\nu_{k,2}(t)-p_1(t)\nu_{k,1}(t), \tag{B6}$$

while the reaction term $w_{k,1}^{(h)}(t)$ (for $k\geqslant 2$) associated with the head of the $(k,1)$-chains is given by Eq. (B2a) with k' set equal to unity. As for isolated chains, the reaction term $w_{1,1}^{(h)}(t)$ [or $w_{1,1}^{(t)}(t)$] is given by Eq. (B5) with $k'=1$ [or Eq. (B6) with $k=1$]. Heretofore, the head and tail of each chain have been distinguished for convenience. Because, in actuality, the middle chain is homogeneous, the subscripts of $\nu_{k,k'}$ are interchangeable: $\nu_{k,k'}(t)=\nu_{k,k'}(t)$. Therefore, the kinetic equation [Eq. (B1)] with the reaction terms given by Eqs. (B2), (B5), and (B6) can be summarized into Eq. (5) with Eq. (6) in the text.

APPENDIX C: RELATION TO THE TANAKA-EDWARDS THEORY

In this appendix, we show that the present theory reduces to the TE theory[22,23] in the limit of a high reduced concentration. Summing Eq. (2) over $2\leqslant k,k'\leqslant s_m$, we obtain

$$\frac{\partial F(\mathbf{r},t)}{\partial t}+\nabla\cdot(\dot{\mathbf{r}}F(\mathbf{r},t))=-2\beta(r)F(\mathbf{r},t)-B_2(t)\sum_{k=2}^{s_m}(F_{k,2}(\mathbf{r},t)+F_{2,k}(\mathbf{r},t))+\left(\sum_{k=1}^{s_m-1}p_k(t)+p_1(t)\right)\nu^d(t)f_0(\mathbf{r}), \tag{C1}$$

where

$$F(\mathbf{r},t)\equiv\sum_{k=2}^{s_m}\sum_{k'=2}^{s_m}F_{k,k'}(\mathbf{r},t) \tag{C2}$$

is the total number of active chains with the head-to-tail vector $\mathbf{r}$ (per unit volume), and

$$\nu^d(t)\equiv\sum_{k=2}^{s_m}(\nu_{k,1}(t)+\nu_{1,k}(t)) \tag{C3}$$

is the total number of dangling chains. (We are assuming that the dissociation rate does not depend on the junction multiplicity, as in the text.) The second term in the right-hand side of Eq. (C1) and p_1 in the third term are related to the annihilation/creation process of pairwise junctions. Let us consider here the case that a small shear deformation is applied to the system, as discussed in the text. Upon integration with respect to $\mathbf{r}$, Eq. (C1) becomes

$$0=-2\beta\left(\nu^{\mathrm{eff}}+\sum_{k=2}^{s_m}\nu_{k,2}\right)+\left(\sum_{k=1}^{s_m-1}p_k+p_1\right)\nu^d. \tag{C4}$$

The terms $\Sigma_{k\geqslant 2}^{s_m}\nu_{k,2}$ and p_1, with regard to pairwise junctions, satisfy the following relation:

$$\frac{\sum_{k=2}^{s_m}\nu_{k,2}}{\nu^{\mathrm{eff}}}=\frac{p_1}{\sum_{k=1}^{s_m-1}p_k}=\frac{q_2}{\alpha}. \tag{C5}$$

As c increases, Eq. (C5) approaches zero as shown in Fig. 9, implying that the pairwise junctions gradually disappear, and hence the right-hand side of Eq. (C4) approaches $-2\beta\nu^{\mathrm{eff}}+(\Sigma_{k\geqslant 1}p_k)\nu^d$. This indicates that Eq. (C1) reduces to

$$\frac{\partial F(\mathbf{r},t)}{\partial t}+\nabla\cdot(\dot{\mathbf{r}}F(\mathbf{r},t))=-2\beta F(\mathbf{r},t)+p\nu^d f_0(\mathbf{r}) \tag{C6}$$

in the high c limit, where

$$p\equiv\sum_{k=1}^{s_m-1}p_k=\beta\frac{\alpha}{q_1} \tag{C7}$$

is the probability that an unassociated group connects to *any* junction per unit time. Equation (C6) is equivalent to the basic equation of the TE theory if isolated chains are absent and p is constant. [2β in the right-hand side of Eq. (C6) is the transition rate from active chains to dangling chains. This quantity is denoted as β in Refs. 22 and 23.]

[1] M. A. Winnik and A. Yekta, Curr. Opin. Colloid Interface Sci. **2**, 424 (1997).
[2] R. D. Jenkins, C. A. Silebi, and M. S. El-Aasser, ACS Symp. Ser. **462**, 222 (1991).
[3] T. Annable, R. Buscall, R. Ettelaie, and D. Whittlestone, J. Rheol. **37**, 695 (1993).
[4] R. D. Jenkins, D. R. Bassett, C. A. Silebi, and M. S. El-Aasser, J. Appl. Polym. Sci. **58**, 209 (1995).
[5] A. Yekta, B. Xu, J. Duhamel, H. Adiwidjaja, and M. A. Winnik, Macromolecules **28**, 956 (1995).
[6] K. C. Tam, R. D. Jenkins, M. A. Winnik, and D. R. Bassett, Macromolecules **31**, 4149 (1998).
[7] O. Vorobyova, A. Yekta, M. A. Winnik, and W. Lau, Macromolecules **31**, 8998 (1998).
[8] Q. T. Pham, W. B. Russel, J. C. Thibeault, and W. Lau, Macromolecules **32**, 2996 (1999).
[9] Q. T. Pham, W. B. Russel, J. C. Thibeault, and W. Lau, Macromolecules

32, 5139 (1999).
[10] W. K. Ng, K. C. Tam, and R. D. Jenkins, J. Rheol. **44**, 137 (2000).
[11] Y. Séréro, V. Jacobsen, J.-F. Berret, and R. May, Macromolecules **33**, 1841 (2000).
[12] S. X. Ma and S. L. Cooper, Macromolecules **34**, 3294 (2001).
[13] S. X. Ma and S. L. Cooper, Macromolecules **35**, 2024 (2002).
[14] D. Calvet, A. Collet, M. Viguier, J.-F. Berret, and Y. Séréro, Macromolecules **36**, 449 (2003).
[15] F. Lafleche, D. Durand, and T. Nicolai, Macromolecules **36**, 1331 (2003).
[16] L. Pellens, R. G. Corrales, and J. Mewis, J. Rheol. **48**, 379 (2004).
[17] L. Pellens, K. H. Ahn, S. J. Lee, and J. Mewis, J. Non-Newtonian Fluid Mech. **121**, 87 (2004).
[18] P. Kujawa, H. Watanabe, F. Tanaka, and F. M. Winnik, Eur. Phys. J. E **17**, 129 (2005).
[19] P. Kujawa, F. Segui, S. Shaban, C. Diab, Y. Okada, F. Tanaka, and F. M. Winnik, Macromolecules **39**, 341 (2005).
[20] P. Kujawa, F. Tanaka, and F. M. Winnik, Macromolecules **39**, 3048 (2006).
[21] A. N. Semenov, J.-F. Joanny, and A. R. Khokhlov, Macromolecules **28**, 1066 (1995).
[22] F. Tanaka and S. F. Edwards, Macromolecules **25**, 1516 (1992).
[23] F. Tanaka and S. F. Edwards, J. Non-Newtonian Fluid Mech. **43**, 247 (1992); **43**, 273 (1992); **43**, 289 (1992).
[24] S. Q. Wang, Macromolecules **25**, 7003 (1992).
[25] G. Marrucci, S. Bhargava, and S. L. Cooper, Macromolecules **26**, 6483 (1993).
[26] A. Vaccarro and G. Marrucci, J. Non-Newtonian Fluid Mech. **92**, 261 (2000).
[27] X.-X. Meng and W. B. Russel, J. Rheol. **50**, 189 (2006).
[28] T. Indei, J. Non-Newtonian Fluid Mech. **141**, 18 (2007).
[29] M. S. Green and A. V. Tobolsky, J. Chem. Phys. **14**, 80 (1946).
[30] T. Indei and F. Tanaka, J. Rheol. **48**, 641 (2004).
[31] T. Indei and F. Tanaka, Nihon Reoroji Gakkaishi **32**, 285 (2004).
[32] W. Binana-Limbele, F. Clouet, and J. Francois, Colloid Polym. Sci. **271**, 748 (1993).
[33] T. Annable, R. Buscall, R. Ettelaie, P. Shepherd, and D. Whittlestone, Langmuir **10**, 1060 (1994).
[34] K. Zhang, B. Xu, M. A. Winnik, and P. M. Macdonald, J. Phys. Chem. **100**, 9834 (1996).
[35] F. Tanaka and W. H. Stockmayer, Macromolecules **27**, 3943 (1994).
[36] T. Indei, J. Chem. Phys. **127**, 144905 (2007).
[37] F. Tanaka and T. Koga, Macromolecules **39**, 5913 (2006).
[38] F. Tanaka and M. Ishida, Macromolecules **29**, 7571 (1996).
[39] D. S. Pearson and W. W. Graessley, Macromolecules **11**, 528 (1978).
[40] The fluctuation of the junctions with a lower multiplicity might be large due to the recoil motion (Ref. 37). The effects of the junction fluctuation will be studied on the basis of the present theory in a forthcoming paper.
[41] If β depends on k, a broader relaxation spectrum will be obtained instead of a single mode. In this series of papers, we employ a constant β as a first approximation, because experimental data show approximately a single relaxation mode.
[42] Equation (13) is also written as $\psi_k = K_k \psi_1$, where $K_k = \gamma_k \lambda^{k-1}$ is the reaction constant.
[43] The same quantity is denoted as p_k in Ref. 35.
[44] They have also considered the minimum junction model (Ref. 35), in which junctions are allowed to take the multiplicity $k=1$ (unassociated) and $k = s_0, s_0+1, \ldots$, for $s_0 \geqslant 2$.
[45] By definition, q_1 must be smaller than or equal to unity.
[46] The fraction of such active chains q_2^2 is rather small in the limit of low c, as we can see from Fig. 9.
[47] In the low c limit, a small number of pairwise junctions exist in the system because $\delta(=0.01)$ is finite. Therefore, the relaxation time is smaller than $1/(2\beta)$ [but greater than $1/(4\beta)$] at $c \sim 0$.